Journal of Applied Polymer Science

Effects of Processing Conditions on Foaming Behaviors of Polyetherimide (PEI) and PEI/Polypropylene Blends in Microcellular Injection Molding Process

Tao Liu, Yajie Lei, Zhenglun Chen, Xianzhong Wang, Shikai Luo
Institute of Chemical Materials, China Academy of Engineering Physics, Mianyang, 621900, People's Republic of China
Correspondence to: T. Liu (E-mail: liutaocaep@163.com) and S. K. Luo (E-mail: luosk_caep@163.com)

ABSTRACT: Foaming behaviors of both neat polyetherimide (PEI) and PEI/polypropylene (PP) blends were studied in this article in microcellular injection molding (Mucell) process. The study mainly focused on the comparison of two materials' foaming behaviors under different processing conditions which took a critical effect on the morphologies of foams. The results indicated that the different characteristics of PEI and PEI/PP blends, such as melt strength, gas dissolvability, and solubility, induced different nucleation ability of PEI and PEI/PP blends. The addition of PP could obviously improve the cell density and reduce the cell size. With the processing conditions changing, the morphologies of PEI/PP altered more variously, and their distribution of cell density was wider. This suggested that foaming behaviors of PEI/PP blends was more flexible to be controlled by the processing conditions than neat PEI. The effects of shot size, gas injection, and injection rate on foam morphologies were studied in detail. Shot size determined the weight reduction of samples and affected the cell density and size significantly. Gas dosing time and dosing rate determined the gas ratio which effected on foam morphologies of the PEI and PEI/PP foams. © 2014 Wiley Periodicals, Inc. J. Appl. Polym. Sci. **2015**, *132*, 41443.

KEYWORDS: blends; foams

Received 25 February 2014; accepted 15 August 2014
DOI: 10.1002/app.41443

INTRODUCTION

Microcellular foams with high cell density of more than 10^8 cells/cm^3 and cell size of less than 100 μm have many excellent characteristics compared with conventional foams with 10^6 cells/cm^3 density and more than 200 μm cell size, such as higher impact stress, less mechanical reduction, and less shrinkage and warpage. Polyetherimide (PEI) has many excellent properties, such as good mechanical behaviors (high specific strength), heat and radiation resistance, and hydrolytic stability, attracting much attention of researchers. It is potential to use the material in aviation industry especially when the mass was considerably reduced by introducing micro cells into it. There are few reports about foaming behaviors of PEI[1,2] in Mucell process with N_2 as blowing agent, most of them were in batch processing with CO_2.

In addition, reports about foaming behaviors of PEI blends with other polymers are few. In fact, foaming of blends is attracting much attention because of multiple characteristics of the blends. The immiscible blends could especially achieve much higher nucleation ability because the interfaces of polymers have lower nucleation energy barrier for bubble nucleation. In immiscible high density polyethylene (HDPE)/polypropylene (PP)[3] blends, the interfacial tension between two phases was very high and made cell nucleate easier, resulting in good foam morphologies.[4–8] By adding 20% of polypheylene ether (PPE) to acrylonitrile-styrene copolymer (SAN),[9] with the action of heterogeneous nucleation, the size of cells reduced significantly. In poly(methyl methacrylate) (PMMA)/PP and polystyrene (PS)/PP blends,[10] PP highly dispersed into the matrix and served as nucleation centers for high diffusivity of blowing agent CO_2 and high interfacial tension with PMMA, resulting in higher cell density and smaller cell size.

On the other hand, in the dual blends, the addition of polymer has an important effect on the dissolvability of CO_2, which can improve the cell density and control the cell morphology. For example, in PS/styrene-butadiene-methyl methacrylate copolymer (SBM) blends,[11] as SBM levels approached 10%, the dissolvability of CO_2 enhanced from 10.4% to 16.9%. In the foaming of polyethylene glycol (PEG)/PS blends,[4] PEG as the dispersed particles were embraced in cells, because the solution and diffusion coefficient of CO_2 in PEG was larger than in PS and cells firstly nucleated in the PEG domains in the initial stage of foaming. With the growth of bubbles in the PEG domains, the bubbles coalesced and eventually embraced the PEG domains because of the low strength of PEG. In PP/

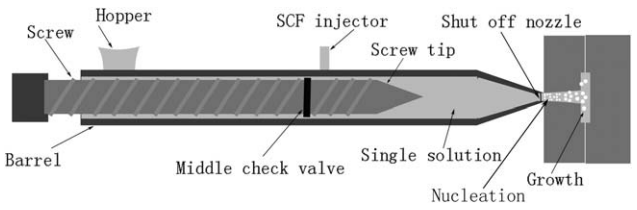

Figure 1. Schematic of the ENGEL Mucell system and foaming processing.

styrene-ethylene-butadiene-styrene copolymer (SEBS),[12] SEBS had lower viscosity and acquired highly dispersed domains in PP. During the foam processing, the bubbles first nucleated in SEBS domains and significantly improved the cell uniformity.

According to these researches, blending with other immiscible polymers with different rheological property could enhance nucleation and change foam morphologies significantly. So far, these researches mainly focused on the batch foaming process with CO_2. However, very little attention is paid to the microcellular injection molding with N_2.

As is well known, the microcellular injection molding is a very effective method to produce excellent dimensional stability parts with lower injection pressure, shorter cycle time, and less material.[13–19] The microcellular injection machine, which is now very popular to make microcellular polymers, is developed and commercialized by Trexel.[20] How to obtain excellent cell structure and morphology is a big challenge, because the melt rheological properties, gas dissolvability, and pressure drop are not as conveniently controlled as batch process. Polymer blending could provide a new way to prepare microcellular foams with much higher cell density and smaller cell size in microcellular injection molding. In this study, foams of PEI and PEI/PP blends with 6 wt % PP were prepared using N_2 as the blowing agent via the Mucell process and the comparative characteristics were studied in detail.

EXPERIMENTAL

Materials

PEI (Ultem 1000), with the class transition temperature (T_g) of 215°C was obtained from Sabic. PP (KF2682), with the T_g of 11°C, was supplied by Andrea Basel. N_2 99.99% in purity was purchased from Chengdu Xin source Chemical Co., Ltd.

Blends Preparation

The PEI resin was firstly dried at 140°C for 4 h to remove residual moisture and then mixed with maleic anhydride grafted polypropylene (PPMA) or PP and processed in a PTW252 twin-screw extruder (HAAKE, Germany) to give samples. The rotational speed of the extruder was 120 rpm, and the temperatures of its eight sections, from the charging hole to the ram head, were 310°C, 320°C, 330°C, 330°C, 335°C, 330°C, 320°C, and 325°C. The samples were dried at 140°C for 4 h to remove moisture and then conventionally injected to standard testing samples.

Microcellular Foams Preparation

Double-shot molding, A VC 330H/80L, supplied by ENGEL (Figure 1) was used to prepare microcellular foams, and supercritical

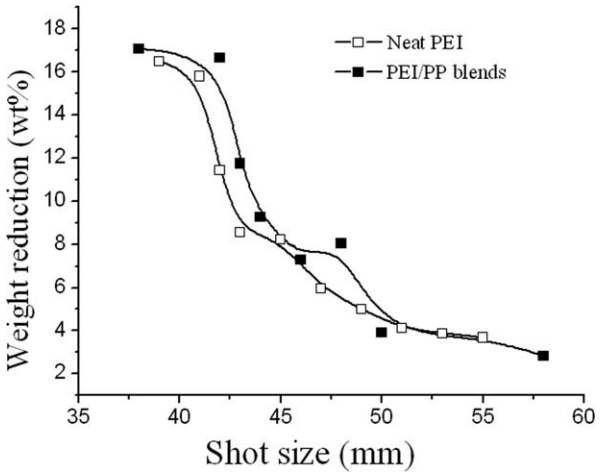

Figure 2. Weight reduction ratio of foamed PEI and PEI/PP blends as a function of shot size.

pumping machine, SII-TR-10, obtained from TREXEL was employed for the conveying of supercritical fluid (SCF) N_2. The temperatures used for the hopper, rear, middle, front, and nozzle positions were 260°C, 280°C, 300°C, 300°C, and 320°C, respectively. The temperature of molded part was 80°C. Melt plasticizing pressure (MPP) was 14 MPa. The following experiments were carried out under these conditions, and focused on the effects of shot size and gas ratio on the morphologies of foams.

Scanning Electron Microscope (SEM) Image Analysis

The samples were fractured after immersing in liquid nitrogen for 20 minutes to keep their original cell morphologies. Quantitative analysis of average cell size and density were determined from SEM images and performed with Nano-Measure 1.2 software. The cell density (N_0), the number of cells per unit volume (cm^3) of the sample was determined from eq. (1):[21]

$$N_0 = \left(\frac{n}{A}\right)^{\frac{3}{2}} \left(\frac{1}{1-V_f}\right) \quad (1)$$

where n is the number of cells in the SEM image, and A is the area of the image (cm^2); V_f is the void fraction of the foamed sample that estimated as:

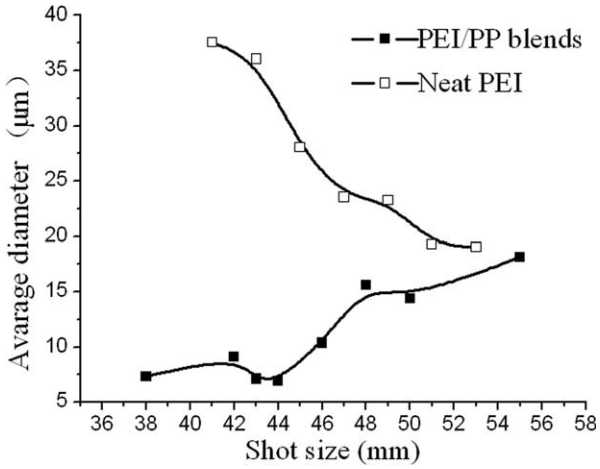

Figure 3. Average cell diameter of foamed PEI and PEI/PP blends as a function of shot size.

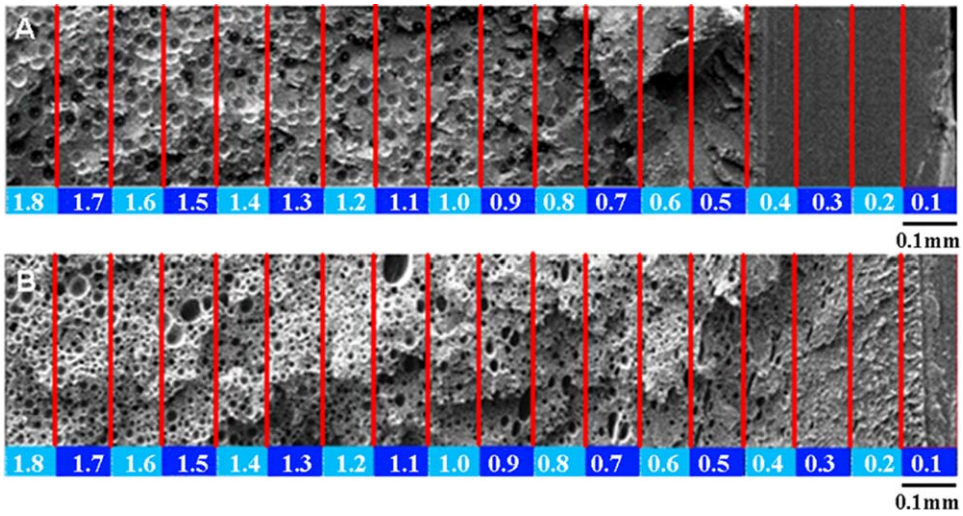

Figure 4. The change of cell size along with the distance to the surface zone. (**A**) microcellular PEI foams, (**B**) microcellular PEI/PP foam (PEI/PP = 94/6). [Color figure can be viewed in the online issue, which is available at wileyonlinelibrary.com.]

$$V_f = 1 - \frac{\rho_f}{\rho} \quad (2)$$

where ρ_f and ρ were the density of foamed and non-foamed samples, respectively.

RESULTS AND DISCUSSION

Shot Size Effect

Figure 2 shows the effect of shot size on weight reduction ratio of the microcellular PEI and PEI/PP foams. The weight reduction ratio decreases with the increase of shot size regularly. Neat PEI and PEI/PP blends show the same tendency. This suggests that the shot size has a critical role to determine the weight reduction in the Mucell process. As the shot size increases above 48 mm, the weight reduction of the microcellular PEI and PEI/PP foams decreases slowly. When the shot size reaches to 48 mm, the volume of melt is exactly the cavity volume of the mold, so the weight reduction is almost invariable. When the shot size is less than 48 mm, the melt cannot fill up the mold, and there will be some space for expanding. The space will be filled up by bubbles confined to the polymer.

In addition, shot size can take an effect on the cell size significantly. Figure 3 illustrates a close correlation between shot size and average size. The microcellular PEI and PEI/PP blends show evidently different tendency as the shot size increases. At low shot size, neat PEI shows much larger cell size than blends. It is due to the lower ability of nucleation for homogenous nucleation. The experimental pressure drop induces insufficient nucleus for neat PEI, and these nucleus share the space to make cavity pressure drop immediately, resulting in stable and large cell size rapidly. However, the number of nucleus induced in PEI/PP blends is evidently larger than that of neat PEI and these nuclei share the space, resulting in a higher cell density and smaller cell size. As the shot size increases, there will be less space for expanding of gas, and the cells of neat PEI have less space to expand which confines cell growth, resulting in smaller size.

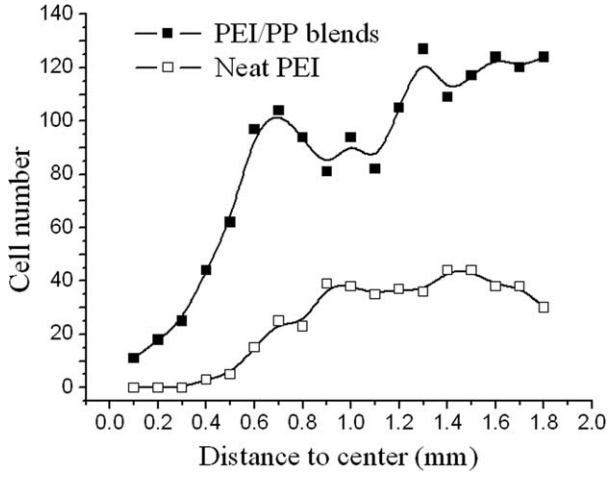

Figure 5. Curves of the cell numbers versus distance for microcellular PEI and PEI/PP foams.

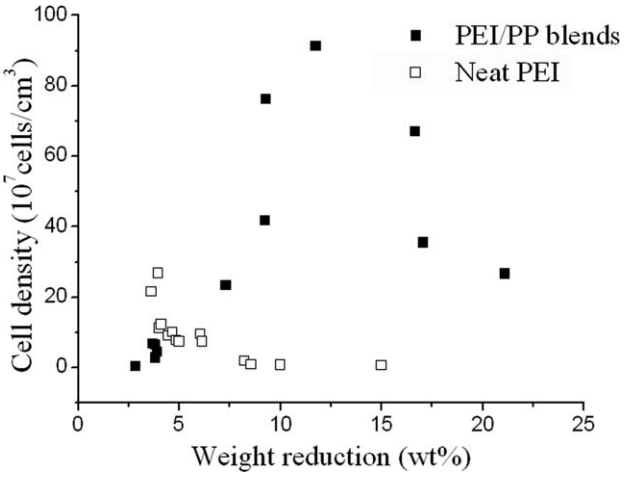

Figure 6. Cell densities of foamed PEI and PEI/PP blends as a function of weight reduction.

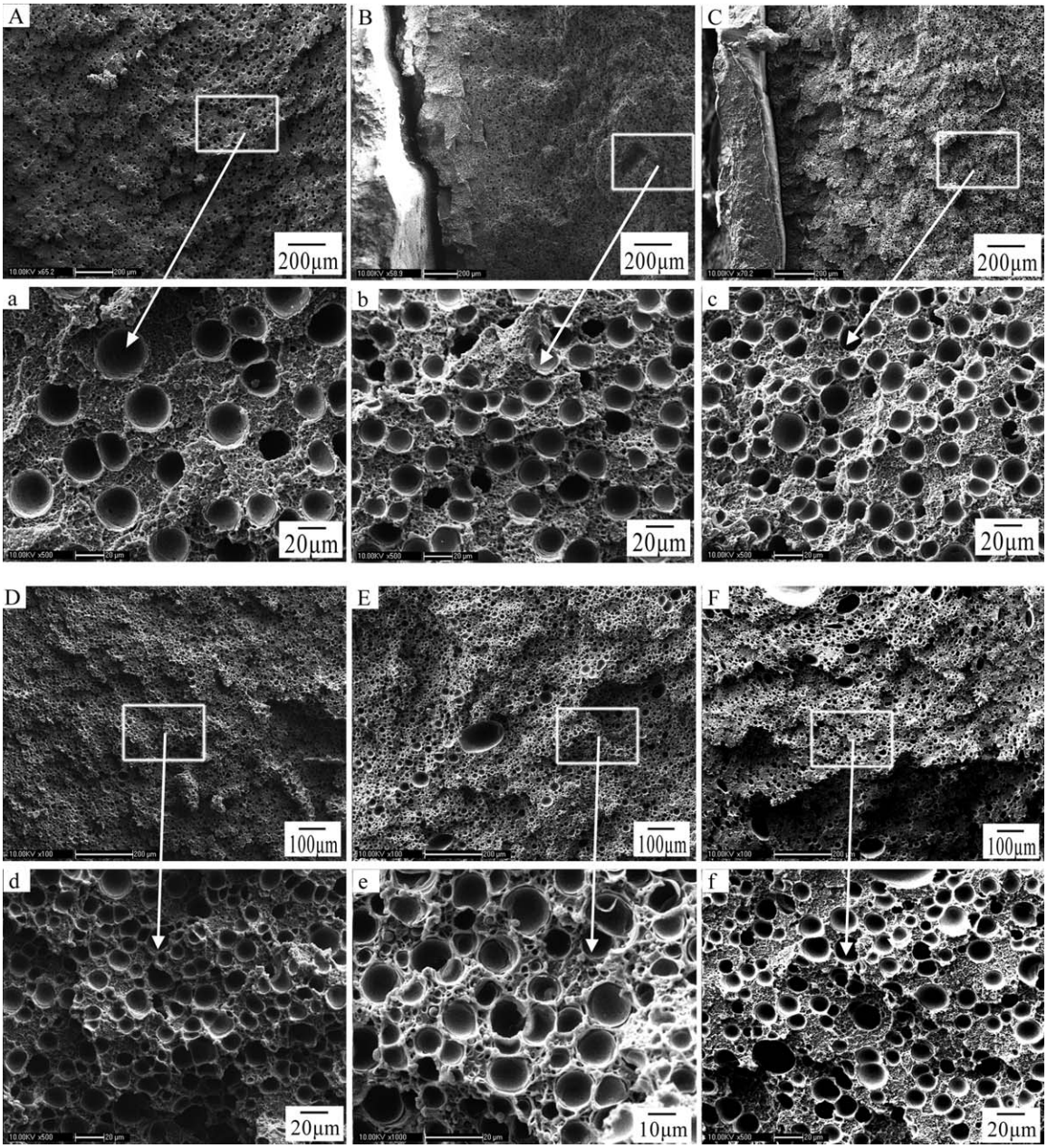

Figure 7. SEM images of foamed PEI/PP blends with different weight reduction ratio: (**a**) 1.98 wt %; (**b**) 3.96 wt %; (**c**) 7.30 wt %; (**d**) 9.24 wt %; (**e**) 16.45 wt %; (**f**) 21.18 wt %.

The cell size of PEI/PP blends is much smaller than PEI when the shot size is below 48 mm. However, when the shot size is larger than 48 mm, their difference is not obvious. This suggests that PEI/PP blends has a higher nucleation ability, providing more nuclei to share the available space, resulting in smaller cell size. When the shot size approaches 48 mm, the cell size of PEI/PP blends become a little bigger, because large number of nuclei cannot grow because of little space to expand to release the pressure in the mold and actually the foaming process is ineffective. The nuclei probably coalesce together and during this period of time lots of gas escape from the mold under the higher cavity pressure. The results indicate that the blends with higher nucleation ability can achieve smaller cells at high expansion space, whereas the neat PEI can achieve smaller cells by little space to confine the cell growth.

From the Figures 4 and 5, one can see that the number of cells in the surface zone is obviously smaller than that of cells in the center zone. Moreover, in the microcellular PEI foams, as the distance reaches 0.4 mm, the cells begin to appear. Compared with the microcellular PEI/PP foams, the distance of appearing cells is just 0.1 mm. The distance of appearing cells is related with two factors. One is the diffusion rate of gas, and other is the nucleation rate of cell. When the diffusion rate is higher than the nucleation rate, the blowing agent reduces because a large number of the gas diffuse from the surface, indicating that

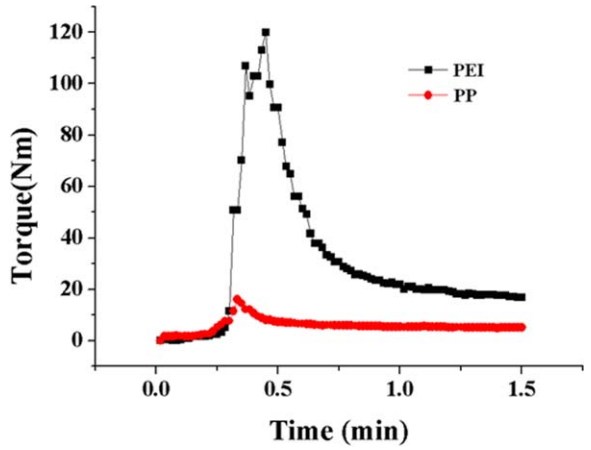

Figure 8. The effect of time on the torque of PEI and PP matrix (the temperature is 330°C). [Color figure can be viewed in the online issue, which is available at wileyonlinelibrary.com.]

the distance of appearing cells increases. When the nucleation rate is higher than the diffusion rate, the distance of appearing cells decreases because the gas has no enough time to diffuse. Therefore, with the addition of PP, the nucleation rate of PEI/PP blends greatly increase, leading to the reduction in the distance. On the other hand, the number of cells in the microcellular PEI/PP foams is greatly higher than that of cells in the microcellular PEI foams. The result proves that the increment of the number of nucleation is because of the presence of PP.

The above analysis indicates that it is convenient to control the weight reduction and cell size by changing the shot size. As shown in Figure 6, the cell density of microcellular PEI/PP foams does not correlate with weight reduction closely. However, as the weight reduction is small (<5 wt %), cell density is very low, and foams of high density usually are achieved between 8 and 18 wt %. Compared with blends, neat PEI shows a narrow distribution of cell density. This suggests that an appropriate weight reduction is required to obtain a smaller cell size and higher cell density foams for neat PEI, but PEI/PP blends can undertake a larger weight reduction.

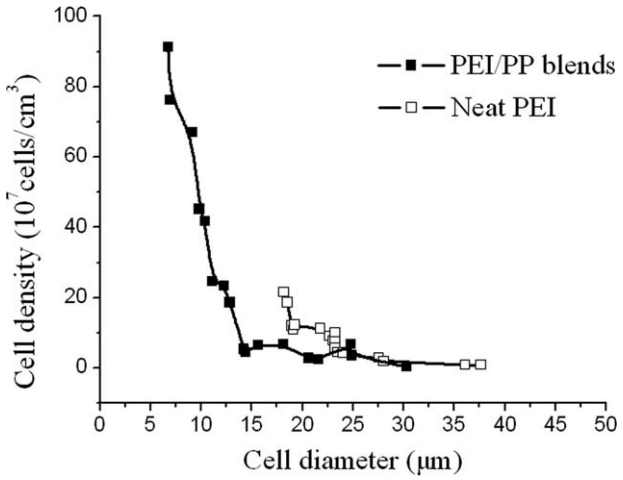

Figure 9. Cell density as a function of cell diameter of foamed PEI and PP/PEI.

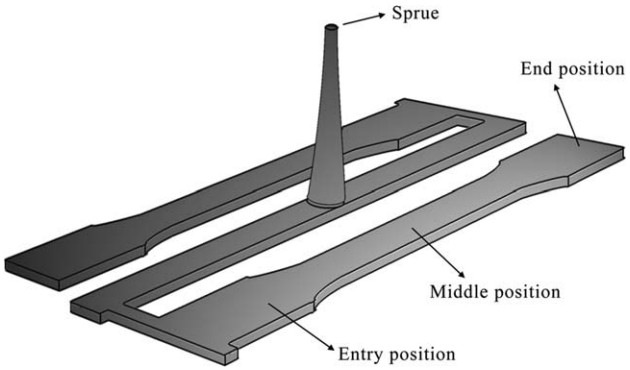

Figure 10. Schematic of the configuration of the molding part.

Figure 7 illustrates the SEM images of foamed PEI/PP with different weight reduction. The foams of 1.98 wt % reduction [Figure 7(a)] has low-density cells, and the non-foamed area occupies the most space. As the reduction increases, the cell density also increases and shows good foam morphologies as shown in Figure 7(c–e).

However, when the weight reduction is over 20 wt %, the cells are less uniform, and there are many much bigger cells distributed among other cells. This is due to too much space provided to cell growth and a lack of appropriate confined stress. Besides the processing of the high expansion can make growing surrounding unstable, resulting in non-uniform cell morphologies. The first nucleated bubbles also grow quickly and more gas is trapped in the matrix, and this can also result in cell coalesce. When the reduction is high enough, the melt expansion even cannot fill up the whole cavity of the mold.

The SEM images of foamed PEI/PP, as illustrated in Figure 7(b,c), have clear surface stripping which is rich in PP, and this is due to the low melt strength of PP as shown in Figure 8. During the melt flowing into the molding, the melt temperature drops quickly, and PP has much lower melt point which keeps flowing easier than PEI, so it will be squeezed out to the surface under high shear stress, resulting in the morphologies like that.

Figure 9 illustrates that both cell density of foamed PEI and PEI/PP blends drop rapidly with the increase of cell size in a definite range. The cell density of foamed PEI and PEI/PP blends keep irregular above 23 and 13 μm, respectively. The lowest cell densities of foamed PEI and PEI/PP blends are nearly equal and the magnitude closed to 10^7 cells/cm^3. This suggests that under the most normal process conditions in Mucell process, the nucleation ability easily kept the magnitude over a definite value. However, the foamed PEI/PP shows a wide range of cell size and density, and achieves much higher cell density. This indicates that by addition of PP to PEI, the blends can easily achieve foams with much higher cell density.

Location Effect

Figure 10 illustrates the configuration of the molding part, and different positions of part will show different morphology of foams. Figure 11 illustrates the morphologies of foams of different positions which are showed in Figure 10. In the end position of sample, during flowing of the melt, the solution has a

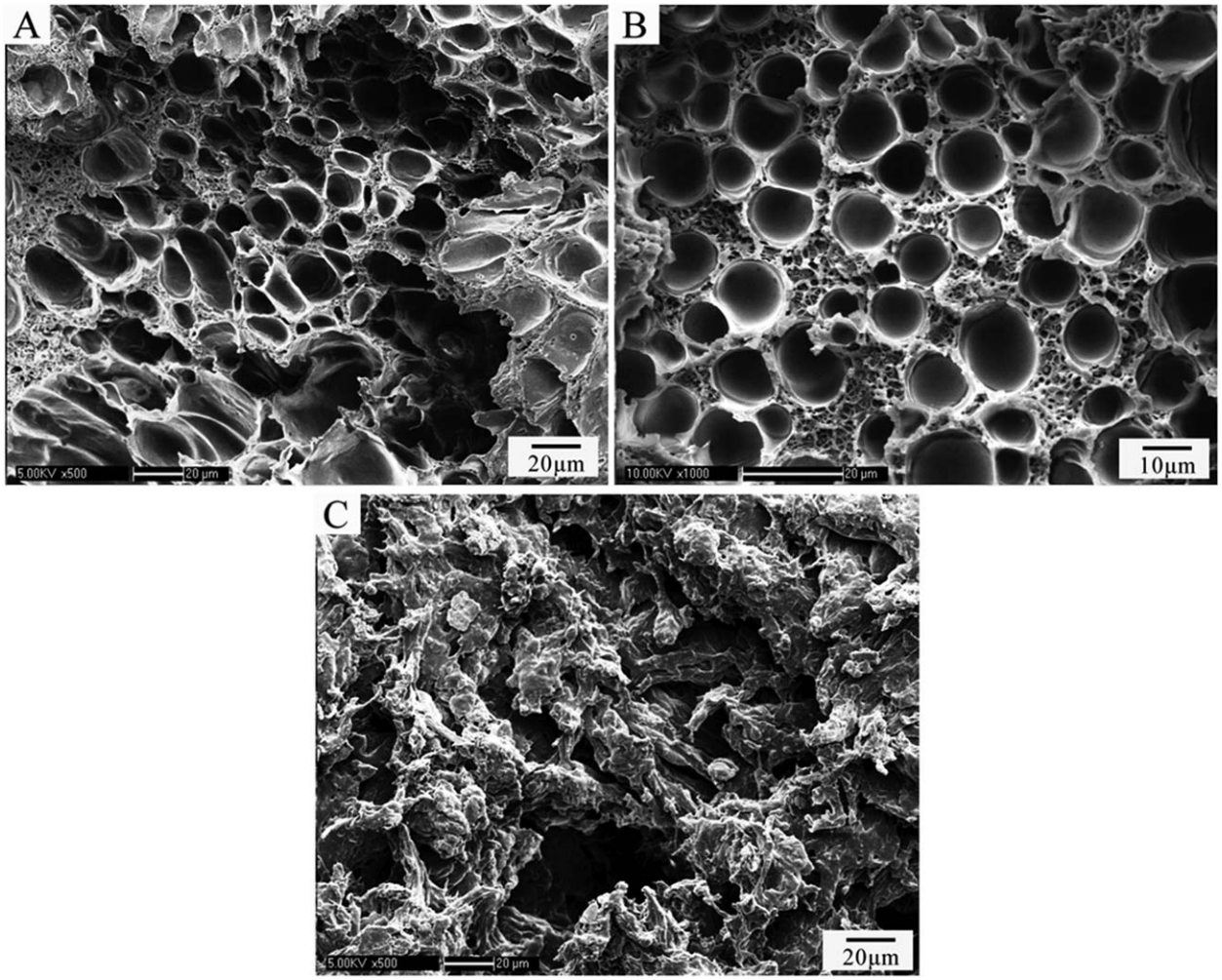

Figure 11. Different positions of molding parts: (**a**) the entry position of the sample; (**b**) middle position of the sample; (**c**) the end position of the sample.

very high pressure drop and enough space, and the growing surroundings is extraordinarily unstable, so the melt cannot confine the gas efficiently. The gas separate out of polymer matrix rapidly, and the polymer may even bust into loosening structures [Figure 11(c)]. The middle position achieves high cell density and regular cells, this is due to the appropriate confined stress and relatively stable growing surroundings [Figure 11(b)]. Entry position shows the close-packed and elliptical cells because of high shear stress, and the cell size is large and not uniform [Figure 11(a)]. The results suggest that it is necessary to design a good mold part to provide appropriate surroundings.

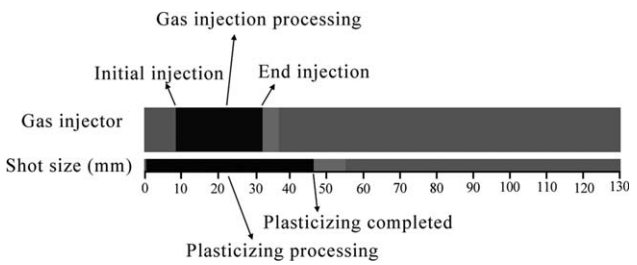

Figure 12. Schematic of plasticizing and gas injection processing.

Gas Injection Effect

There are two parameters to control the magnitude of SCF gas injected into barrel: injecting time (t) and gas dosing rate (v). The weight ratio (R) of gas to melt determined from eq. (3):

$$R = \frac{V \times t}{W} \tag{3}$$

where W is the melt weight injected into barrel. The initial dosing time can change by different positions of plasticizing processing (Figure 12), and take different effects on the melt. The plasticizing time in the following experiments kept 16 seconds which is more than gas dosing time.

Figure 13 illustrates the morphologies of foamed blends, the gas ratio is concluded in the Table I. Figure 13(A) shows that when the gas ratio is 0.19 wt %, the cell density is low, and most of the area is non-foamed. This ratio of gas can be absolutely dissolved into melt, but the melt with low ratio of gas results in low nucleation ability. With the increase of gas ratio, the cell

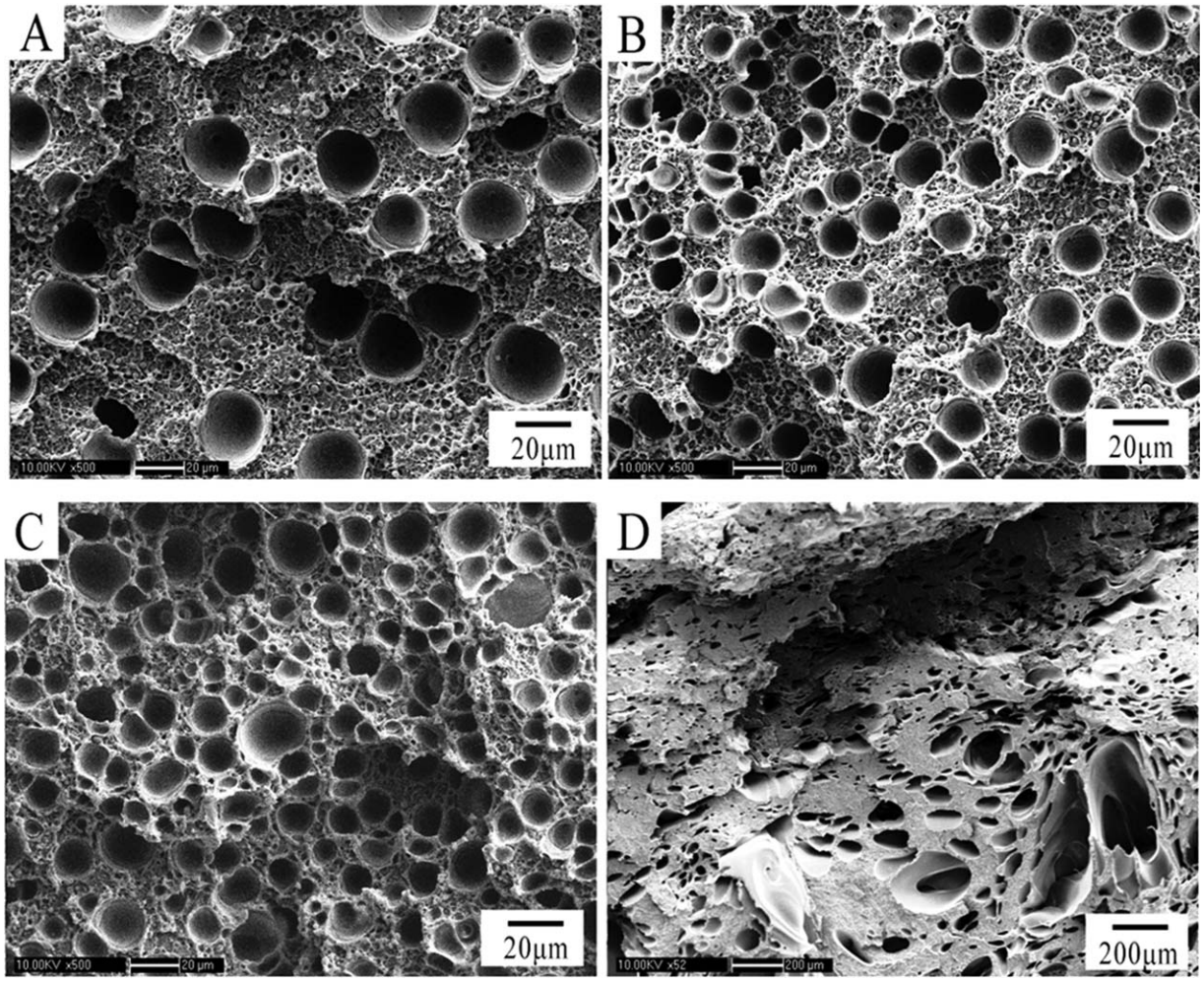

Figure 13. SEM images of foamed PEI/PP blends with 0.09 kg/h of gas dosing rate, and different dosing time and gas ratio: (**A**) 3 s and 0.19 wt %; (**B**) 6 s and 0.39 wt %; (**C**) 10 s and 0.64 wt %; (**D**) 15 s and 0.96 wt %.

density increases evidently [Figure 13(A,B)]. Whereas when the ratio reaches 0.96 wt %, the cells deform sharply and become very big in partial area. This is due to much gas cannot dissolve into melt and directly expand to be cells. These cells are big enough and shaped like ellipsoid by the shear stress on the way of filling the mold.

Figure 14(A,B) shows a low cell density for the gas ratio is low. The conditions are concluded in Table II. The cell density improves with the increase of gas ratio. Figure 14(C,D) illustrate that the cells are much more uniform and close-packed, showing good cell morphologies. This suggests that the gas dissolves in the melt totally, forming a gas-melt single solution. However when the ratio increase further, cells become less uniform, and the cells deviated from center are deformed greatly by the shear stress, because the gas injected into the melt exceeds its solubility and exists as air bubbles in the melt, and they are easy to be deformed to different shape which is much bigger than the cells nucleated from single solution. Figure 14(E) illustrates that the cells near the skin deform severely and they are almost flat or nearly broken. Figure 14(F) has only 3 seconds' gas injection, and this suggests that the time is too short to make gas dissolve totally and uniformly into the melt, resulting in foaming of local gas rich area and very large cells partially. With the action of shear stress, the melt with rich gas will arrange as circles around the core.[14] Thus cells show an arc surrounding the core. The sample of Figure 14(G) enhances the time to 8 seconds, and the ratio is more than 1 wt %. Under the condition, more gas cannot dissolve into the melt and most of cells are directly expanded from the separated air bubbles in the melt, and this will also make much gas escape from the mold.

In addition, neat PEI is foamed with different gas dosing rate, the gas ratio range from 0.26 to 0.82 wt % (Table III). Figure 15(A,B) show that as the gas ratio is lower than 0.39, the

Table I. Gas Ratio (R) Changes with the Same Gas Dosing Rate (v)

Sample	A	B	C	D
t (s)	3	6	10	15
v (kg/h)	0.09	0.09	0.09	0.09
R (wt %)	0.19	0.39	0.64	0.96

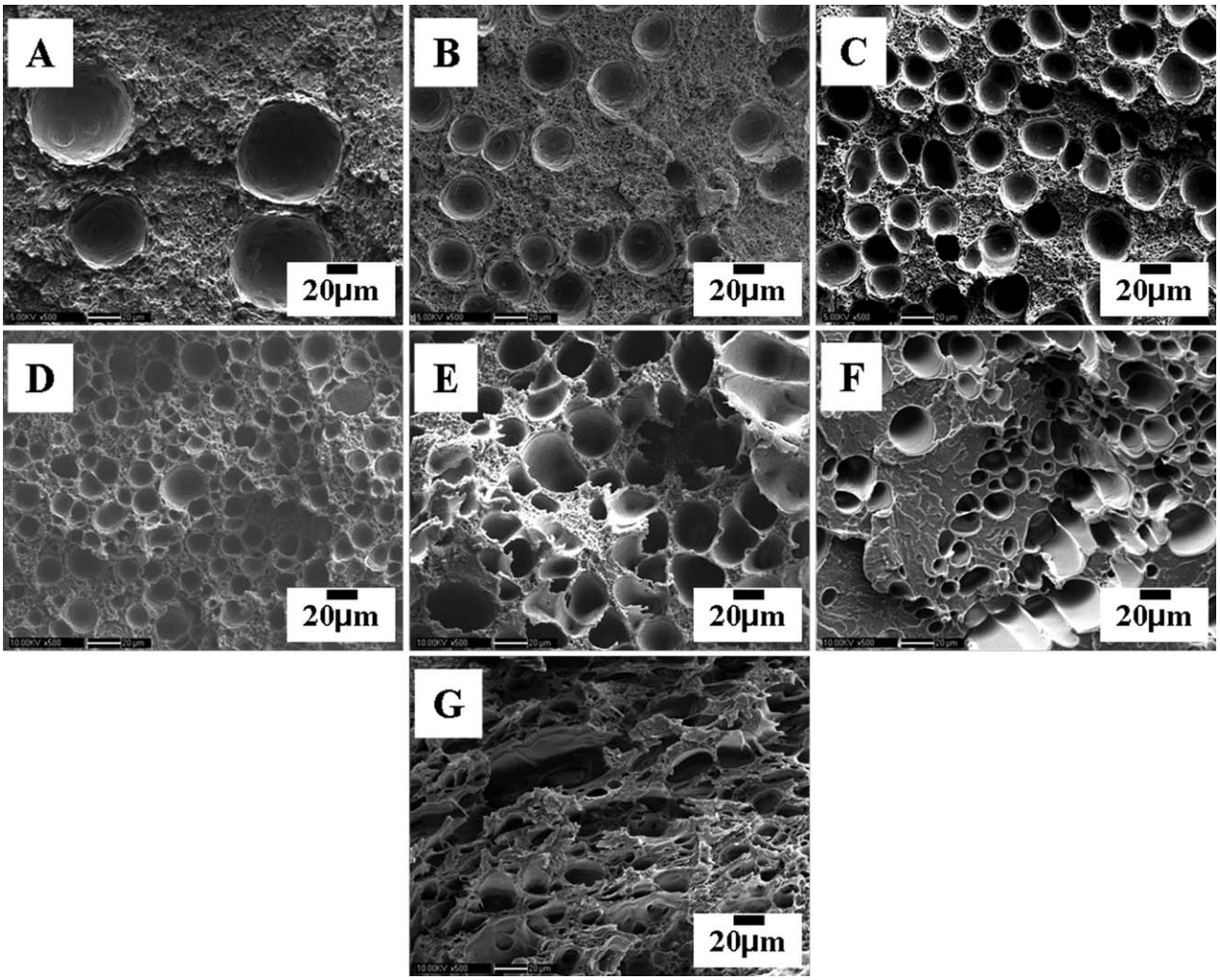

Figure 14. SEM images of foamed PEI/PP blends with different dosing time, gas dosing rate, and gas ratio: (**A**) 6 s, 0.03 kg/h, and 0.13 wt %; (**B**) 6 s, 0.06 kg/h, and 0.26 wt %; (**C**) 6 s, 0.09 kg/h, and 0.39 wt %; (**D**) 6 s, 0.12 kg/h, and 0.51 wt %; (**E**) 6 s, 0.19 kg/h, and 0.82 wt %; (**F**) 3 s, 0.19 kg/h, and 0.41 wt %; (**G**) 8 s, 0.19 kg/h, and 1.09 wt %.

cells are spherical and had a relatively uniform distribution. However as the gas ratio increases over 0.39 wt % [Figure 15(C)], the cells distributes widely and cell shape deforms clearly, this suggests that much gas cannot dissolve into melt. When gas ratio reaches 0.82 wt %, cells totally deform and they are formed directly from air bubble rather than nucleate from single solution.

The experiments with different gas dosing rate and dosing time are discussed above, which suggest that gas ratio below 0.51 wt % could well dissolves into melt of PEI/PP blends, obtaining the gas-melt single solution, and the ratio around 0.50 wt % achieves the best cell morphologies. However in neat PEI, the morphologies become worse when gas ratio is over 0.39 wt %, and the cell density of PEI is lower than PEI/PP significantly. This is due to the dissolvability of N_2 in PP blends is higher than that of PEI.

So the results also suggest that the gas dosing time cannot be too short that covers only a short period of time during plasticizing, which will result in non-uniform dissolution and eventually affects the distribution of cells.

Table II. Gas Ratio (R) Changes with Different Gas Dosing Time (t), Dosing Rate (v)

Sample	A	B	C	D	E	F	G
t (s)	6	6	6	6	6	3	8
v (kg/h)	0.03	0.06	0.09	0.12	0.19	0.19	0.19
R (wt %)	0.13	0.26	0.39	0.51	0.82	0.41	1.09

Table III. Gas Ratio (R) Changes with the Same Dosing Time (t) and Different Gas Dosing Rate (v)

Sample	A	B	C	D
t (s)	6	6	6	6
v (kg/h)	0.06	0.09	0.12	0.19
R (wt %)	0.26	0.39	0.51	0.82

Injection Rate Effect

Figure 16 illustrates the cell density of foamed PEI increases with the increase of injection rate, whereas the PEI/PP blends is irregular as a function of injection rate. Many reports show that the increase of injection rate can increase the drop pressure, which is favorable to nucleation.[20] In neat PEI, nucleation ability is the dominate factor that affects cell density, however PEI/PP blends has a higher nucleation ability and pressure drop is less important. This will make it more sensitive for neat PEI to injection rate than PEI/PP blends.

Most of differences of foaming behaviors between neat PEI and PEI/PP blends talked above are due to their different nucleation ability. The surface tension of PP is lower than PEI at experimental temperature and the dissolvability in PP is higher than in PEI, which make gas much easier nucleate in PP domains. What's more, their interface provides much zone of lower nucleation energy barrier, so PEI/PP blends shows a higher ability of nucleation.

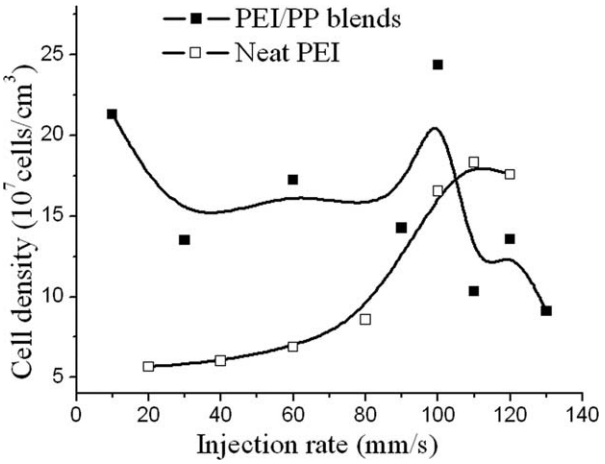

Figure 16. Cell densities of foamed PEI and PEI/PP blends as a function of injection rate.

CONCLUSIONS

The study investigated the foaming behaviors of neat PEI and PEI/PP blends with 6 wt % PP in microcell injection molding process, and the blends achieved much higher cell density and smaller cell size. The shot size made a critical role to determine the weight reduction of sample, and both neat PEI and PEI/PP blends showed the same tendency. However the shot size had

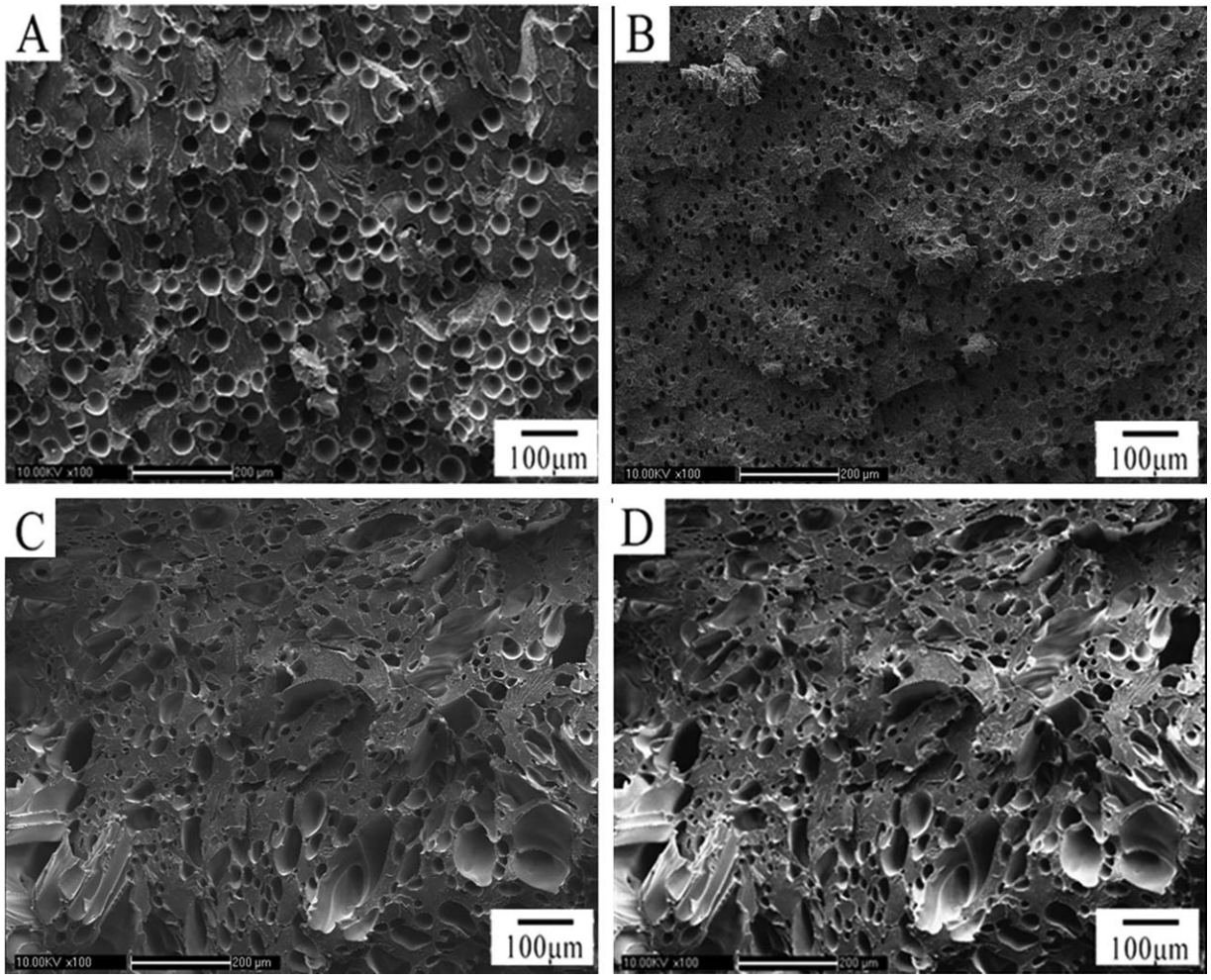

Figure 15. SEM images of foamed neat PEI with different gas dosing rate and gas ratio: (**A**) 0.06 kg/h and 0.26 wt %; (**B**) 0.09 kg/h and 0.39 wt %; (**C**) 0.12 kg/h and 0.51 wt %; (**D**) 0.19 kg/h and 0.82 wt %.

the different effects on two materials, which was due to their different nucleation ability, diffusivity and solubility. The results show that appropriate weight reduction was required to make a higher cell density.

The foam morphologies of different processing conditions, such as gas dosing time, gas dosing rate, and injection rate of melt were studied in detail, and foamed PEI showed much lower cell density and smaller cell size than PEI/PP blends. By comparing the morphology of different gas ratio, neat PEI showed a low solubility of N_2 than PEI/PP blends. With the processing conditions changing, the morphologies of PEI/PP altered more variously, and their distribution of cell density was wider. Foaming behaviors of PEI/PP blends was more flexible to be controlled by the processing conditions than neat PEI. This suggested that it is very potential to make variously foamed products by blending with other polymers.

ACKNOWLEDGMENTS

We acknowledge financial support from Science and Technology Development Foundation of China Academy of Engineering Physics (Grant number: 2013B0302041).

REFERENCES

1. Nemoto, T.; Takagi, J.; Ohshima, M. *Polym. Eng. Sci.* **2010**, *50*, 2408.
2. Miller, D.; Kumar, V. *Polymer* **2011**, *52*, 2910.
3. Rachtanapun, P.; Selke, S. E.; Matuana, L. M. *Polym. Eng. Sci.* **2004**, *44*, 1551.
4. Taki, K.; Nitta, K.; Kihara, S. I.; Ohshima, M. *J. Appl. Polym. Sci.* **2005**, *97*, 1899.
5. Ramesh, N. S.; Rasmussen, D. H.; Campbell, G. A. *Polym. Eng. Sci.* **1994**, *34*, 1685.
6. Zhai, W.; Yu, J.; Wu, L.; Ma, W.; He, J. *Polymer* **2006**, *47*, 7580.
7. Spitael, P.; Macosko, C. W.; McClurg, R. B. *Macromolecules* **2004**, *37*, 6874.
8. Tatiboue, J.; Gendron, R.; Hamel, A.; Sahnoune, A. *J. Cell. Plast.* **2002**, *38*, 203.
9. Ruckdäschel, H.; Rausch, J.; Sandler, J. K.; Altstädt, V.; Schmalz, H.; Müller, A. H. *Polym. Eng. Sci.* **2008**, *48*, 2111.
10. Sharudin, R. W.; Nabil, A.; Taki, K.; Ohshima, M. *J. Appl. Polym. Sci.* **2011**, *119*, 1042.
11. Ruiz, J. A. R.; Marc-Tallon, J.; Pedros, M.; Dumon, M. *J. Supercrit. Fluid.* **2011**, *57*, 87.
12. Sharudin, R. W. B.; Ohshima, M. *Macromol. Mater. Eng.* **2011**, *296*, 1046.
13. Chandra, A.; Gong, S.; Turng, L.; Gramann, P. *J. Cell. Plast.* **2004**, *40*, 371.
14. Kramschuster, A.; Cavitt, R.; Turng, L. S.; Chen, Z. B. *Plast. Rubber Compos.* **2007**, *46*, 198.
15. Yoon, J. D.; Cha, S. W.; Chong, T. H.; Ha, Y. W. *Polym. Plast. Technol. Eng.* **2007**, *46*, 815.
16. Shen, C.; Kramschuster, A.; Ermer, D.; Turng, L. S. *Int. Polym. Process.* **2006**, *21*, 393.
17. Hidetomo, H.; Tomoki, M.; Masami, O.; Satoshi, Y.; Hiroshi, H. *Mater. Sci. Eng. C* **2010**, *30*, 62.
18. Hwang, S. S.; Liu, S. P.; Hsu, P. P.; Yeh, J. M. *Int. Commun. Heat. Mass. Transfer* **2011**, *38*, 1219.
19. Jungjoo, L.; Lih, S. T.; Eugene, D.; Patrick, G. *Polymer* **2011**, *52*, 1436.
20. Xu, J. Microcellular Injection Molding; Wiley: New Jersey, **2011**.
21. Kumar, V.; Suh, N. P. *Polym. Eng. Sci.* **1990**, *30*, 1323.